INTERNATIONAL JOURNAL FOR NUMERICAL METHODS IN FLUIDS
Int. J. Numer. Meth. Fluids 2009; **60**:1315–1333
Published online 17 October 2008 in Wiley InterScience (www.interscience.wiley.com). DOI: 10.1002/fld.1932

Numerical study of an inviscid incompressible flow through a channel of finite length

Vasily N. Govorukhin[1,*,†] and Konstantin I. Il'in[2]

[1]*Southern Federal University, Rostov-on-Don, Russia*
[2]*Department of Mathematics, University of York, Heslington, York YO10 5DD, U.K.*

SUMMARY

A two-dimensional inviscid incompressible flow in a rectilinear channel of finite length is studied numerically. Both the normal velocity and the vorticity are given at the inlet, and only the normal velocity is specified at the outlet. The flow is described in terms of the stream function and vorticity. To solve the unsteady problem numerically, we propose a version of the vortex particle method. The vorticity field is approximated using its values at a set of fluid particles. A pseudo-symplectic integrator is employed to solve the system of ordinary differential equations governing the motion of fluid particles. The stream function is computed using the Galerkin method. Unsteady flows developing from an initial perturbation in the form of an elliptical patch of vorticity are calculated for various values of the volume flux of fluid through the channel. It is shown that if the flux of fluid is large, the initial vortex patch is washed out of the channel, and when the flux is reduced, the initial perturbation evolves to a steady flow with stagnation regions. Copyright © 2008 John Wiley & Sons, Ltd.

Received 20 June 2007; Revised 21 July 2008; Accepted 21 August 2008

KEY WORDS: particle methods; Galerkin method; partial differential equations; time integration; Euler flow; incompressible flow; flow through a given domain

1. INTRODUCTION

Flows through a given domain with an inflow and outflow of the fluid have attracted the attention of many researchers because of their relevance to many problems of natural sciences and engineering, e.g. blowing ventilation of rooms and tunnels, problems of transport and control of environmental pollution, flows through pipes and ducts of finite length. In many situations, an inviscid incompressible flow through a given domain with permeable boundary is the simplest

*Correspondence to: Vasily N. Govorukhin, Department of Mathematics, Southern Federal University, Milchakova str. 8a, Rostov-on-Don 344090, Russia.
†E-mail: vgov@math.rsu.ru

Contract/grant sponsor: EPSRC; contract/grant number: GR/S96616/02
Contract/grant sponsor: RFBR; contract/grant numbers: 07-01-92213, 08-01-00895
Contract/grant sponsor: CRDF; contract/grant number: RUM1-2842-RO-06

Copyright © 2008 John Wiley & Sons, Ltd.

appropriate model of a real flow. The corresponding initial boundary-value problem requires an additional boundary condition at the inlet, where the fluid enters the flow domain. The first formulation of the corresponding mathematical problem is due to Kochin [1], who proposed to specify the vorticity at the inlet in addition to the normal velocity (which is given both at the inlet and the outlet). Yudovich [2] had shown that in the two-dimensional case this problem has a unique global (in time) solution. However, in the three-dimensional case this problem is ill-posed. To get a well-posed initial boundary-value problem, it is necessary to specify either the tangent velocity or the tangent vorticity (in addition to the normal velocity) at the inlet [3]. Steady inviscid flows through a given domain had been studied in [4], where it had been shown that a steady two-dimensional problem with the vorticity prescribed at the inlet has at least one solution for arbitrary (time-independent) boundary data. In general, such flow may contain stagnation (recirculation) region, which may consist of several disconnected parts. Fluid particles remain in the stagnation region forever. The rest of the flow domain is always connected, and each fluid particle stays in this part of the flow domain only for a finite time interval.

Two-dimensional inviscid flows with stagnation (recirculation) regions have been studied both analytically and numerically by many authors. Examples include a flow past a circular cylinder [5], free-surface flows past an obstacle on the bottom [6], and many other flows (see [7]). Viscous flows with stagnation regions in a channel of finite length have been also studied numerically (see, e.g. [8] and references there).

Inviscid flows with stagnation regions in a channel of finite length, with the normal velocity given at both ends of the channel and vorticity prescribed at the inlet, have hardly been studied at all. Such flows without stagnation zones were considered in [9], where wide classes of asymptotically stable (in the linear approximation) flows had been found. Steady flows in a curved channel, satisfying the same boundary conditions, had been treated in [10]. In that paper, steady flows without stagnation zones had been found and the effect of the channel curvature is investigated. As far as we are aware, unsteady flows have not been studied numerically yet.

It should be noted that the problem of an inviscid flow through a given domain is not conservative. Fluid particles bring along the energy and vorticity when they enter the flow domain and take them away when they leave it [2, 9]. This makes possible the phenomena (such as asymptotic stability, self-oscillations, etc.), which are typical for dissipative systems but unusual for inviscid flows. Note that the dissipation inside the flow domain is absent, so that the purely conservative dynamics can be observed in stagnation zones if they are present. From the computational viewpoint, the presence of dissipation can considerably simplify the numerical solution of the problem without stagnation zones, whereas many numerical difficulties are still present for flows with stagnation zones.

In numerical simulations of inviscid incompressible flows, various forms of the so-called vortex method (see [11, 12] and references there) are employed. Convergence and error bounds for this method had been established in [11, 13–15]. The vortex method is especially popular when the flow domain is the entire plane, because in this case the velocity can be easily found from the vorticity using Green's function of the Poisson equation [16, 17]. In the case of a closed flow domain or a channel, the problem is more complicated because one needs to solve the Poisson equation numerically. In this paper, we describe a numerical method for solving the initial boundary-value problem for the Euler equations in the rectangular channel, with normal velocity given at both the inlet and the outlet and vorticity prescribed at the inlet. We study the dynamics of an initial vortex patch for various flow rates through the channel. The main result of the paper is that, under certain conditions, a stable steady flow with stagnation zones can appear as a result of the temporal evolution of an initial flow.

Copyright © 2008 John Wiley & Sons, Ltd.

DOI: 10.1002/fld

2. GOVERNING EQUATIONS AND NUMERICAL METHOD

We consider an inviscid incompressible flow through a rectangular channel D as:

$$D=\{(x,y):0\leqslant x\leqslant L;0\leqslant y\leqslant 1\} \tag{1}$$

The Euler equations written in terms of stream function and vorticity have the form

$$\omega_t+\psi_y\omega_x-\psi_x\omega_y=0 \tag{2}$$

$$-(\psi_{xx}+\psi_{yy})=\omega \tag{3}$$

Here, $\psi_x=\partial\psi/\partial x$, $\psi_y=\partial\psi/\partial y$, $\psi_{xx}=\partial^2\psi/\partial x^2$, etc. The velocity of the fluid $\mathbf{v}=(v_1,v_2)$ is expressed via the stream function ψ as

$$v_1=\psi_y \tag{4}$$

$$v_2=-\psi_x \tag{5}$$

We assume that the side of the rectangle at $x=0$ is the flow inlet, and the side at $x=L$ is the outlet (see Figure 1), i.e.

$$v_1(x,y)|_{x=0}>0,\quad v_1(x,y)|_{x=L}>0 \tag{6}$$

Possible boundary and initial conditions for Equations (2)–(3) have been discussed in [2, 3] (see also [18]). Here, we employ the boundary conditions proposed by Yudovich [2]; in addition to the normal velocity that is prescribed both at the inlet and at the outlet, which we specify as the vorticity at the inlet. We will consider only the case where the normal velocity profiles at the inlet and the outlet are the same, i.e. $v_1|_{x=0}=v_1|_{x=L}$. This leads to the following boundary conditions for ψ and ω:

$$\psi|_{x=0}=\psi|_{x=L}=\psi^w(y),\quad y\in[0,1] \tag{7}$$

$$\omega|_{x=0}=\omega^w(y) \tag{8}$$

Here, ω^w is an arbitrary function of $y\in(0,1)$, and ψ^w is an increasing function of $y\in(0,1)$. Since the stream function is defined up to a constant, we choose $\psi^w(y)$ such that $\psi^w(0)=0$. Boundary condition (7) means that the fluid flows into and out of the channel with the same normal velocity $v_1|_{x=0}=v_1|_{x=L}=v^w(y)=\mathrm{d}\psi^w(y)/\mathrm{d}y$ (see Figure 1). The restriction that ψ^w is an increasing function of y ensures that conditions (6) are satisfied. At the rigid walls of the channel, the standard conditions of no normal velocity are specified as: $v_2|_{y=0}=v_2|_{y=1}=0$. These conditions imply that the stream function ψ must be constant at $y=0$ and $y=1$. The additional requirement that the boundary conditions at the rigid walls are consistent with boundary conditions at the inlet and outlet leads to the following boundary conditions for ψ:

$$\psi|_{y=0}=0,\quad \psi|_{y=1}=\psi^w(1) \tag{9}$$

In addition to the boundary conditions (7)–(9), the following initial condition for vorticity should be posed at time $t=0$:

$$\omega|_{t=0}=\omega_0(x,y) \tag{10}$$

Copyright © 2008 John Wiley & Sons, Ltd.

DOI: 10.1002/fld

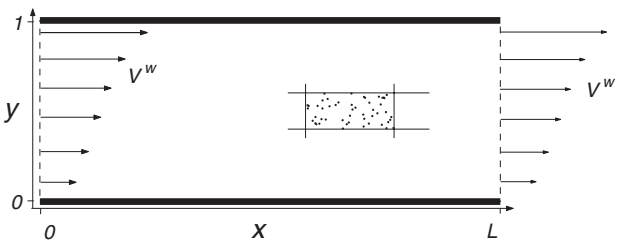

Figure 1. The computational domain and an example of a cell with particles used to approximate function $\omega(x, y)$.

It has been shown in [2] that the initial boundary-value problem (2), (3), (7)–(10) always has a global (in time) unique solution.

Problem (2), (3), (7)–(10) has steady solutions, which correspond to flows without stagnation regions. Their stability was studied in [9], where wide classes of linearly asymptotically stable flows were found. One of these asymptotically stable flows is the flow with linear velocity profile and constant vorticity, given by

$$\omega = -2Q_2, \quad \psi = Q_1 y + Q_2 y^2 \tag{11}$$

where Q_1 and Q_2 are arbitrary constants. In this case, $\omega^w = -2Q_2$ and $\psi^w(y) = Q_1 y + Q_2 y^2$. When $Q_2 = 0$, we obtain the flow with constant velocity and zero vorticity.

The main aim of this paper is the numerical solution of the initial boundary-value problem (2), (3), (7), (8), (10) for various initial conditions (10) and functions ω^w and ψ^w.

One of the most popular methods of numerical solution of Equations (2), (3) is the particle (vortex) method. There are many versions of this method (see, e.g. [11]). Function $\omega(x, y)$ at each moment of time t is approximated by its values in fluid particles having the coordinates $(x_i(t), y_i(t))$. This is a reasonable assumption because Equation (2) implies that the vorticity is passively advected by the velocity field (v_1, v_2), so that the initial value of the vorticity in a particle is conserved with time: $\omega(x_i(t), y_i(t)) = \omega_0(x_i(t_0), y_i(t_0))$. Stream function is determined from Equation (3), and the motion of fluid particles obeys the equations

$$\dot{x}_i = \psi_y(x_i, y_i) = v_1, \quad \dot{y}_i = -\psi_x(x_i, y_i) = v_2 \tag{12}$$

The main difference between various versions of the particle method is in the way of solving Equation (3). In the particle-in-cell method, Equation (3) is solved using one of the standard techniques (finite-difference methods [12] or spectral methods [19]). Then, the stream function is used to compute the trajectories of the fluid particles $(x_i(t), y_i(t))$. It is this approach that is employed in the present study. An alternative method uses expressions of the form $\psi(x, y) = \int_D G(x - x', y - y')\omega(x', y')\,dx'\,dy'$, where G is Green's function. In this case, various quadrature formulae are employed to compute the stream function (see [16, 17]). However, this approach requires an explicit formula for Green's function.

It is convenient to present ψ as

$$\psi = \Psi + \psi^w \tag{13}$$

Copyright © 2008 John Wiley & Sons, Ltd.

DOI: 10.1002/fld

Then Equation (3) takes the form

$$-(\Psi_{xx}+\Psi_{yy})=\omega+\psi^w_{yy} \tag{14}$$

and the boundary condition for Ψ becomes

$$\Psi|_{x=0}=\Psi|_{x=L}=\Psi|_{y=0}=\Psi|_{y=1}=0 \tag{15}$$

Now the equations of motion of the particles (12) have the form

$$\dot{x}_i=\Psi_y(x_i,y_i)+\psi^w_y, \quad \dot{y}_i=-\Psi_x(x_i,y_i) \tag{16}$$

To solve the problem (14), (15) for each t, we employ the Galerkin method. With the basis functions

$$g_{ij}=\sin\left(\frac{\mathrm{i}\pi x}{L}\right)\sin(\mathrm{j}\pi y) \tag{17}$$

we seek a solution in the form

$$\Psi\approx\widetilde{\Psi}=\sum_{i=1}^{k_x}\sum_{j=1}^{k_y}\Psi_{ij}g_{ij} \tag{18}$$

After substitution of (18) into Equation (14) and the standard operation of projection of the solution on the basis functions, we obtain the following expression for the coefficients Ψ_{ij}:

$$\Psi_{ij}=\frac{4L}{\pi^2(i^2+L^2j^2)}\left[\int_0^L\int_0^1\omega(x,y)\sin\left(\frac{\mathrm{i}\pi x}{L}\right)\sin(\mathrm{j}\pi y)\,\mathrm{d}x\,\mathrm{d}y\right.$$

$$\left.+\int_0^L\int_0^1\psi^w_{yy}(y)\sin\left(\frac{\mathrm{i}\pi x}{L}\right)\sin(\mathrm{j}\pi y)\,\mathrm{d}x\,\mathrm{d}y\right] \tag{19}$$

Note that the factor before the expression in square brackets rapidly goes to zero as $i,j\to\infty$. This makes it possible to use a fairly small number of terms in the sum (18). If function $\psi^w(y)$ is sufficiently simple, the second integral in Equation (19) can be found analytically. For a complicated function $\psi^w(y)$, this can be done numerically. In any case, this does not lead to any serious difficulty. Thus, the problem of finding the coefficients in (18) reduces to calculating the integrals

$$I_{ij}=\int_0^L\int_0^1\omega(x,y)\sin\left(\frac{\mathrm{i}\pi x}{L}\right)\sin(\mathrm{j}\pi y)\,\mathrm{d}x\,\mathrm{d}y \tag{20}$$

The main difficulty here is to approximate $\omega(x,y)$. In this paper, we partition the domain D in $N_{\mathrm{box}}=n_x\times n_y$ rectangular cells (see Figure 1). In each cell, function $\omega(x,y)$ is approximated by a polynomial $\phi_k(x,y)$ of degree 3 in x and y as:

$$\omega(x,y)\Big|_{k\text{th cell}}\approx\phi_k(x,y)=\sum_{i,j=0,i+j\leqslant 3}^{3}a_{kij}x^iy^j \tag{21}$$

Copyright © 2008 John Wiley & Sons, Ltd.

DOI: 10.1002/fld

Application of similar cubic polynomials to some problems of dynamics of an inviscid incompressible fluid was discussed in [20]. To find the coefficients a_{kij} in each cell, we use the method of least squares. In most test examples, this method produces considerably better results than interpolation techniques. Thus, to determine the unknown coefficients a_{kij}, we minimize the following expression:

$$S_k = \sum_m \left(\sum_{i,j=0, i+j\leqslant 3}^{3} a_{kij} x^i y^j - \omega(x_m, y_m) \right)^2 \tag{22}$$

Here, the summation is performed over all particles in the kth cell, and $\omega(x_m, y_m)$ is the value of vorticity in the mth particle. To find all coefficients a_{kij}, we solve N_{box} systems of 10 linear algebraic equations, which is not too expensive in terms of computational complexity. When a_{kij} are found, we easily compute integrals (20). In doing this we use an analytical expression for I_{ij}, and this considerably reduces the computation time.

For each particle we solve Equations (16). After finding coefficients Ψ_{ij}, the discrete velocity field $\tilde{v} = (\tilde{v_1}, \tilde{v_2})$ is given by

$$\tilde{v_1} = \dot{x}_i = \sum_{i=1}^{k_x} \sum_{j=1}^{k_y} \Psi_{ij} \frac{\partial g_{ij}}{\partial y} + \psi_y^w, \quad \tilde{v_2} = \dot{y}_i = -\sum_{i=1}^{k_x} \sum_{j=1}^{k_y} \Psi_{ij} \frac{\partial g_{ij}}{\partial x} \tag{23}$$

Initially, we place $N_p(k)$ particles in the kth cell. The initial distribution of particles can be chosen arbitrarily (e.g. randomly) and it is not necessarily uniform. The vorticity in each particle is determined from the initial condition (10). During the computation, the total number of particles $N_p = \sum_k N_p(k)$ is kept unchanged. If a particle leaves the computational domain, we add a new particle at the inlet, and the vorticity in this particle is prescribed in accordance with the boundary condition (8). Thus, the total number of particles remains constant.

One of the key requirements for a numerical approximation of differential equations is that the approximation should preserve certain properties of the original problem. For the two-dimensional dynamics of an inviscid incompressible fluid, the main computational problem is to guarantee the conservation of area by the flow (or, equivalently, the conservation of the incompressibility of the velocity field) [21]. It can be shown that the approximation in the form (23) preserves the incompressibility condition (12).

Property 1

The discrete velocity field (23) preserves the incompressibility of the original velocity field (12).

Partial derivatives of the discrete velocity field are

$$\frac{\partial \tilde{v_1}}{\partial x} = \sum_{i=1}^{k_x} \sum_{j=1}^{k_y} \Psi_{ij} \frac{\partial^2 g_{ij}}{\partial y \partial x}, \quad \frac{\partial \tilde{v_2}}{\partial y} = -\sum_{i=1}^{k_x} \sum_{j=1}^{k_y} \Psi_{ij} \frac{\partial^2 g_{ij}}{\partial x \partial y}$$

Evidently, the divergence of the velocity $\tilde{v}$ is zero at any point of the domain D as:

$$\frac{\partial \tilde{v_1}}{\partial x} + \frac{\partial \tilde{v_2}}{\partial y} = 0 \tag{24}$$

Moreover, Equations (23) represent a Hamiltonian system with the Hamilton function $\tilde{\Psi} + \psi^w$, given by (18). A very important property of Hamiltonian systems is the conservation of the volume

Copyright © 2008 John Wiley & Sons, Ltd.

DOI: 10.1002/fld

in the phase space (which in the present case is equivalent to the conservation of the mass of the fluid) with time. Operators that have this property are called symplectic. It is known that all explicit numerical methods for solving initial value problems for Hamiltonian systems break the symplecticity of the original system, although methods with high accuracy may approximately preserve this property for long time [22]. One of the ways to overcome this difficulty is to employ the symplectic integrators which preserve this property. However, these symplectic integrators are implicit and, in practice, cannot be applied to the problem considered here. In [23, 24] explicit methods have been proposed, which preserve the symplecticity with the accuracy higher than the accuracy of the numerical solution itself. In the following section, we present the results of a comparative study of solving Equation (16) by the Runge–Kutta (RK) method of order four and by the pseudo-symplectic method PS36 [23] that has the third-order accuracy of the numerical solution and the sixth-order accuracy in preserving the simplecticity of the system. These test calculations demonstrate the effectiveness of using pseudo-symplectic integrators for solving the problem considered here.

As mentioned above, problem (2)–(10) has dissipative properties, which makes possible the existence of asymptotically stable flow regimes. A long time unsteady evolution of an initial perturbation may result in a steady flow regime. Unfortunately, in long-time numerical calculations, we cannot make the effect of numerical errors small. This is especially true when steady regimes that appear as a result of long-time evolution of the flow contain stagnation (recirculation) zones. Since the dynamics in these zones is conservative, perturbations of the flow produced by numerical errors are accumulated in these zones. Therefore, if we are interested in finding steady regimes with stagnation zones, we should eliminate these perturbations and find a steady vorticity distribution, which is close to the distribution obtained by a long-time numerical computation.

To do this we employ the following procedure:

1. The vorticity distribution obtained as a result of long-time computation of the unsteady problem is averaged in space as follows. The flow domain is divided in rectangular cells (for the rectangular flow domain D (Figure 1) with $L=3$, the cells are squares with side 0.05). The particles in each cell are used to compute the averaged value of the vorticity. As a result, we obtain an averaged vorticity field.
2. The fast Fourier transform in x and y is applied to the averaged vorticity. In the Fourier spectrum that obtained all small coefficients (the coefficients whose magnitude is smaller than 0.1% of the maximum coefficient) are discarded. This effectively leads to the elimination of spatial modes with high wave numbers and makes the vorticity distribution smooth.
3. Further, we apply the inverse Fourier transform to obtain a new smoothed vorticity distribution.
4. The new vorticity distribution is used as initial data (10) for a new long time (upto $t=1000$) computation of the unsteady problem.
5. Computation of the steady regime is stopped, if a long-time computation of the unsteady problem yields the vorticity distribution whose difference from the initial distribution does not exceed 0.01%. If the difference is greater than 0.01%, the whole procedure is repeated.

Thus, the problem of finding a steady flow regime is reduced to a search for a new initial vorticity distribution (10), which does not change with time. By applying the above procedure

Copyright © 2008 John Wiley & Sons, Ltd.

DOI: 10.1002/fld

we have found non-trivial steady regimes of a flow of an inviscid incompressible fluid through a rectangular domain.

3. TESTING OF NUMERICAL METHOD

As was mentioned before, from a computational viewpoint, the problem of numerical simulation of an inviscid incompressible flow through a channel is easier than numerical simulation of a flow in a closed domain because of the presence of dissipation. Therefore, to test the computational algorithm described above, we consider examples of numerical calculation in the worst case—in a closed rectangular domain D in the absence of a flow through its boundary. In this case, we set

$$\psi^w(y) \equiv 0, \quad \omega^w(y) \equiv 0 \tag{25}$$

in the boundary conditions (7)–(9), i.e. the normal velocity is zero.

The aim of the numerical calculations described below is to test the accuracy and the adequacy of the calculations based on the proposed numerical algorithm in various situations. We analyze the dependence of the results on both the spatial discretization and the time step. For the problem of solving the system of ordinary differential equations (23), we compare the two methods: the RK method of order four (RK4) and the pseudo-symplectic integrator PS36 that has third-order accuracy of the numerical solution and preserves the symplecticity of the system with sixth-order accuracy. Note that one step of the RK4 method requires four evaluations of the right-hand side of the equation, whereas the PS36 method uses five evaluations. Therefore, in the RK4 calculations we use the time step $h_{\mathrm{RK4}} = \frac{4}{5} h_{\mathrm{PS36}}$, where h_{PS36} is the time step in the PS36 method. This choice guarantees that the two methods require the same computational resources for the same time intervals.

To measure the adequacy of calculations, we study the conservation of the integral of the vorticity over the flow domain $I_\omega = \int_D \omega(x, y)\,\mathrm{d}x\,\mathrm{d}y$, which is conserved in time (in the case of a closed domain).

In the test examples, where the exact formula for the velocity $\mathbf{v}_{\mathrm{ex}}(x, y)$ of fluid particles is known we additionally compute the maximum magnitude of the deviation of the computed velocity $\mathbf{v}(x, y)$ from its exact value $\varepsilon_v = \max_{i=1..N_p} \|\mathbf{v}(x_i, y_i) - \mathbf{v}_{\mathrm{ex}}(x_i, y_i)\|$.

3.1. Stationary regimes

Calculation of a steady regime is a standard way to test a numerical scheme for solving unsteady boundary-value problems for partial differential equations. Even for dissipative systems of ordinary differential equations of low dimensions, it is well known that if the initial conditions correspond to an unstable steady regime, then the numerical solution will move away from this regime irrespective of the accuracy of the numerical methods employed. This is a consequence of the roundoff errors that are present in any numerical calculation and which may be treated as small random perturbations of the unstable steady regime. This phenomenon is more clearly seen in conservative systems and systems with large number of dimensions. In the case of a stable steady regime, and especially in the presence of dissipation, these difficulties are practically absent.

Copyright © 2008 John Wiley & Sons, Ltd.

DOI: 10.1002/fld

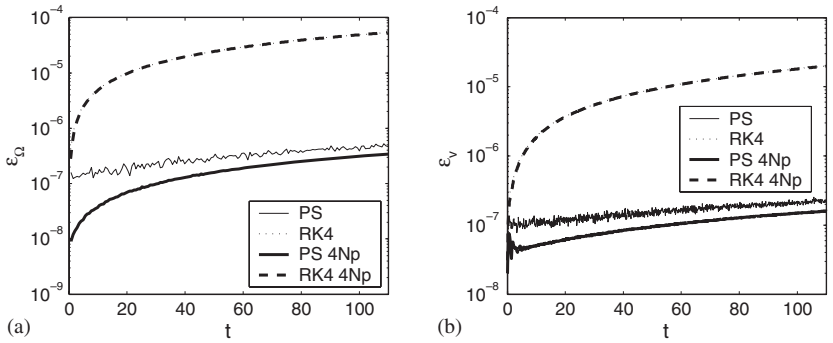

Figure 2. The errors in calculation of the steady regime (26) with $A=0.2, m_x=m_y=1$: (a) for the integral of the vorticity I_ω and (b) for the maximum deviation of the computed velocity from its exact value ε_v. The time steps are $h_{\mathrm{PS}}=0.1$, $h_{\mathrm{RK4}}=0.4/5$. Thin curves correspond to calculations with $N_p=20\,000$ particles, and thick curves to $N_p=80\,000$.

To test the effectiveness of the proposed numerical algorithm, we consider the following steady regime:

$$\psi(x,y)=A\sin(m_x\pi x/L)\sin(m_y\pi y),\quad \omega(x,y)=\frac{(m_x^2+m_y^2L^2)\pi^2}{L^2}\psi(x,y)$$
$$v_1=Am_y\pi\sin(m_x\pi x/L)\cos(m_y\pi y),\quad v_2=-A\frac{m_x\pi}{L}\cos(m_x\pi x/L)\sin(m_y\pi y) \tag{26}$$

where A, m_x, m_y are constants.

Steady flow (26) is stable for $A=0.2$ and $m_x=m_y=1$, and unstable for $A=0.2/9$ and $m_x=m_y=3$. Both cases correspond to the same value of the maximum of the vorticity in the flow domain. In the test calculations we are interested in (i) to what extent the quantities I_ω and ε_v are conserved with time and (ii) which of the above numerical schemes is better in this respect. The test calculations are carried out for the rectangular domain D (Figure 1), with $L=1$ and for two cases of spatial discretization: $n_x=n_y=20$ and $n_x=n_y=40$. At an initial time, each cell contains 50 particles, so that the total number of particles are 20 000 and 80 000, respectively.

The results of the test calculations of the stable steady flow (26), which employ two different methods for solving the equation of motion of the particles (with the time step $h=0.1$ for the method PS36 and with $h=\frac{0.4}{5}$ for RK4) and two different discretizations in space, are shown in Figure 2. One can see that the pseudo-symplectic integrator PS36 yields considerably better results for all considered quantities than the RK4. In addition to this, the results obtained by the method PS36 are visibly improved if a finer spatial discretization is used. Note that the refinement of spatial discretization does not improve the calculations by the RK method, because the dominating error comes from the violation of the incompressibility condition in the RK method. In other words, the refinement of spatial discretization has a smaller effect on the error than the change in the phase volume at each time step. The method PS36 conserves the phase volume better than the RK method and therefore, a finer spatial discretization leads to a clearly visible reduction of error.

In the case of the unstable flow (26), the situation becomes worse (see Figure 3). For a sufficiently long-time interval the considered quantities remain almost unchanged, but the accumulating numerical errors force the system to leave the steady regime. A fourfold increase in the number

Copyright © 2008 John Wiley & Sons, Ltd.

DOI: 10.1002/fld

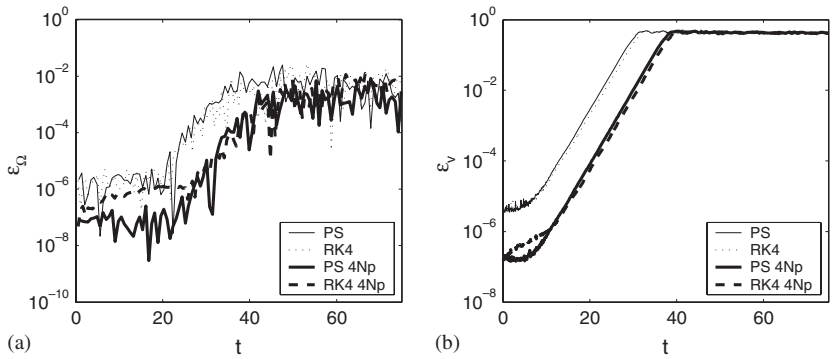

Figure 3. The errors in calculation of the steady regime (26) with $A=0.2/9, m_x=m_y=3$: (a) for the integral of the vorticity I_ω and (b) for the maximum deviation of the computed velocity from its exact value ε_v. The time steps are $h_{\mathrm{PS}}=0.1$, $h_{\mathrm{RK4}}=0.4/5$. Thin curves correspond to calculations with $N_p=20000$ particles, and thick curves to $N_p=80000$.

of cells and accordingly, in the number of particles does not lead to a considerable increase of the time interval within which the numerical solution remains close to the steady regime. In this case, the method PS36 produces result comparable with those produced by RK4.

Similar calculations are also carried out for the steady regimes (11). It turns out that for all the values of parameters Q_1 and Q_2 and for sufficiently small time step h both methods almost exactly reproduce this regime. In this case, the presence of the dissipation of energy leads to an improved effectiveness of the methods.

The above-described test calculations demonstrate the effectiveness of the use of the pseudo-symplectic integrator for numerical simulations of inviscid incompressible flows through a given domain.

3.2. Evolution of elliptic vorticity distribution

To test the proposed numerical algorithm further, we carry out a number of calculations of the evolution of an initially elliptic vortex patch in the absence of inflow and outflow through the boundary of the domain. Similar studies have been done before, for example, in the case where the flow domain is the whole plane [16] or a circle [25].

We solve Equations (2)–(3) in a square with side $L=3$, subject to the boundary condition (15) with $\omega^w=\psi^w(y)=0$. The initial vortex patch is given by $\omega(x,y)|_{t=t_0}=\mathrm{e}^{-45(x-3/2)^2-5(y-3/2)^2}$. We use the method PS36 with time step $h_{\mathrm{PS}}=0.1$ on the interval $t\in[0,350]$, the number of particles is $N=45000$, and the step sizes of spatial discretization are $h_x=h_y=0.1$. The computed distributions of vorticity corresponding to several moments of time are shown in Figure 4. These results are in a qualitative agreement with known results (see, e.g. [16, 25]). In these calculations, the relative error in calculation of quantity I_ω does not exceed 2% for the whole time interval.

These calculations of the evolution of the elliptic vortex patch are employed to experimentally determine the number of the terms in expansion (18) that is sufficient for adequate calculations. To do this, the calculations are carried out in two cases as: $k_x=k_y=20$ and $k_x=k_y=40$. The two-fold increase in the number of terms of the expansion in each spatial variable practically does

Copyright © 2008 John Wiley & Sons, Ltd.

DOI: 10.1002/fld

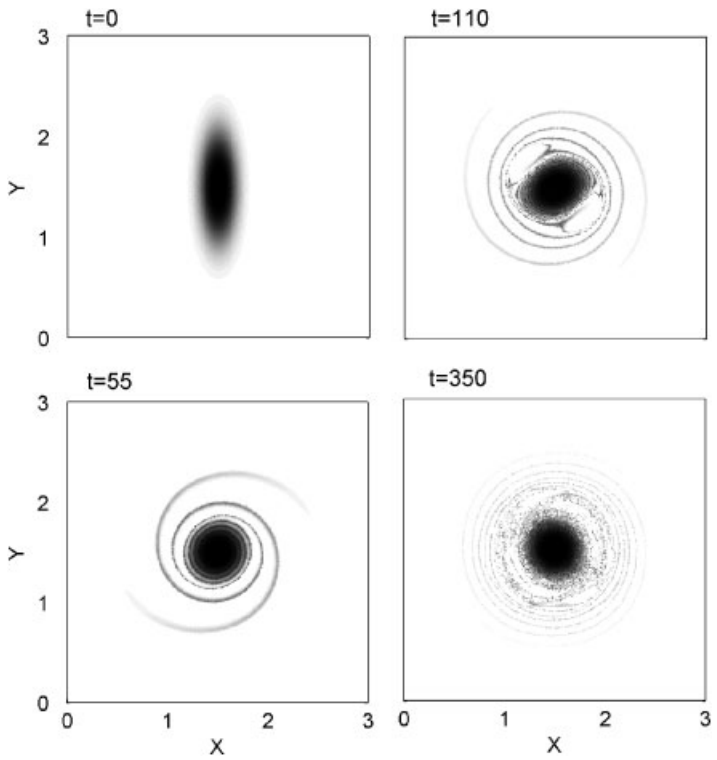

Figure 4. Evolution of an elliptic vortex patch.

not affect the results. Figure 5 shows the maximum magnitudes of Galerkin's coefficients Ψ_{ij} for $i, j = 1, 2, \ldots, 20$ over the time interval $t \in [0, 350]$. One can see that low harmonics dominate, whereas the contribution of higher harmonics is small. This observation allows us to assume that for adequate numerical calculations in similar situations for inviscid flows through a given domain (with a non-zero normal flow through the boundary), it is sufficient to take $k_x = 15$ and $k_y = 15$ in expansion (18). This assumption is reasonable because, from the computational viewpoint, simulations of flows with non-zero normal velocity at the boundary (for similar time intervals and similar domain size) is an easier task due to the presence of dissipation.

4. NUMERICAL RESULTS

The above-described numerical scheme is applied to the numerical simulation of the evolution of a vortex patch in an inviscid flow through a rectangular channel. The aim of the calculations is to study the dynamics of the vortex patch and its dependence on the velocity at the inlet v^w and to investigate the possibility and the mechanism of formation of flows with stagnation zones.

We solve the system of Equations (2)–(3) numerically with initial conditions (10) and boundary conditions (7)–(8). The simplest boundary conditions are chosen: the constant normal velocity $v^w = Q_1$ both at the inlet and the outlet and zero vorticity at the inlet. The boundary conditions

Copyright © 2008 John Wiley & Sons, Ltd.

DOI: 10.1002/fld

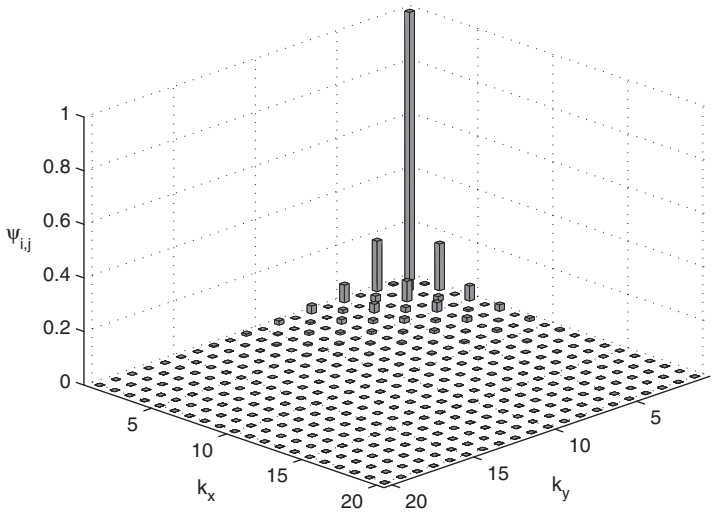

Figure 5. Maximum values of coefficients Ψ_{ij} in the expansion (18) obtained in calculation of the evolution of an elliptic vortex patch.

have the form:

$$\psi|_{x=0}=\psi|_{x=L}=\psi^w(y)=Q_1 y, \quad Q_1>0, \quad y\in[0,1] \tag{27}$$

$$\psi|_{y=0}=0; \quad \psi|_{y=1}=Q_1 \tag{28}$$

$$\omega|_{x=0}=\omega^w(y)=0 \tag{29}$$

These boundary conditions and the zero initial condition for the vorticity, $\omega_0(x, y)=0$, correspond to the steady flow with constant velocity (11). It is known that small perturbations to this steady flow decay to zero for a finite time interval. However, available theoretical results do not say what the practical meaning of the term 'small perturbation' is. Neither they answer the questions on what happens when perturbations are not small, and whether the flow can evolve towards other steady regimes if the initial perturbations are sufficiently large.

In all the numerical experiments described below, we consider the rectangular channel D (1) with the horizontal side $L=3$. The initial vorticity is given by

$$\omega_0(x, y)=\mathrm{e}^{-45(x-3/4)^2-15(y-1/2)^2} \tag{30}$$

The normal velocity at the inlet and the outlet $v^w=Q_1$ is varied in the interval $Q_1\in[0, 0.1]$.

On the basis of the results of the test calculations (see Section 3) we employ cubic functions of the form (21) to approximate function $\omega(x, y)$. For solving the initial value problem for Equations (12), we use the pseudo-symplectic integrator PS36. In numerical calculations we use mainly the following values of the parameters of the method:

number of fluid particles $N_p=48\,000$;
number of terms in expansion (18): $k_x=k_y=15$;
partition of the rectangle in $N_{\mathrm{box}}=1200$ cells ($n_x=60, n_y=20$);
step size in time $h=0.1$.

Copyright © 2008 John Wiley & Sons, Ltd.

DOI: 10.1002/fld

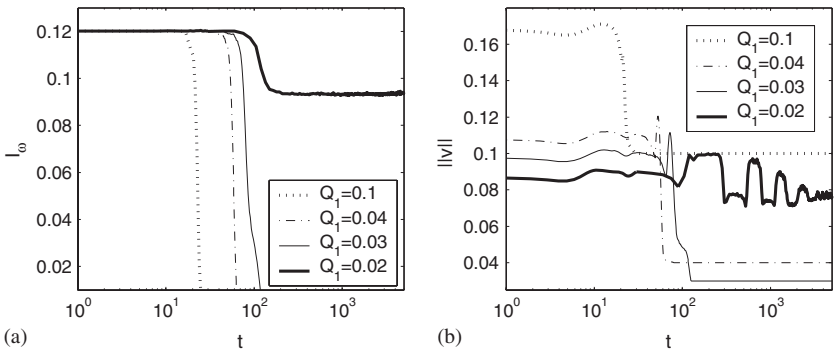

Figure 6. (a) The integral of vorticity over the flow domain I_ω versus time. (b) The maximum magnitude of the velocity in the flow domain versus time.

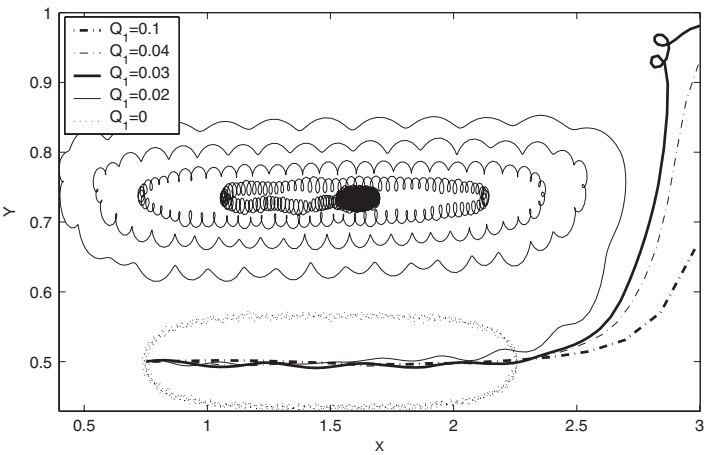

Figure 7. Trajectory of the particle corresponding to maximum vorticity for various values of the inlet velocity $Q_1 \in [0, 0.1]$.

Remark

To further verify the correctness of numerical results, in a number of calculations, we used a higher number of particles $N_p = 108\,000$, a higher number of terms $k_x = k_y = 20$ in Equation (18), smaller cells ($n_x = 90, n_y = 30$), and a smaller time step $h = 0.05$. These calculations were carried out for two values of the parameter Q_1: $Q_1 = 0.1, 0.02$, and on the time interval $t \in [0, 200]$. In both cases, these refined calculations lead to practically the same results as the calculations with the above standard values of the parameters of the method.

The results are presented in graphic form. In the figures where the vorticity is shown, black colour corresponds to the maximum vorticity (equal to unity), white colour corresponds to the minimum (zero) vorticity. Figure 6 shows the vorticity integral (over D) I_ω and the maximum velocity as functions of time for various values of parameters. The trajectory of the particle that corresponds to the maximum vorticity is shown in Figure 7 for various values of the inlet velocity $Q_1 \in [0, 0.1]$.

Copyright © 2008 John Wiley & Sons, Ltd.

DOI: 10.1002/fld

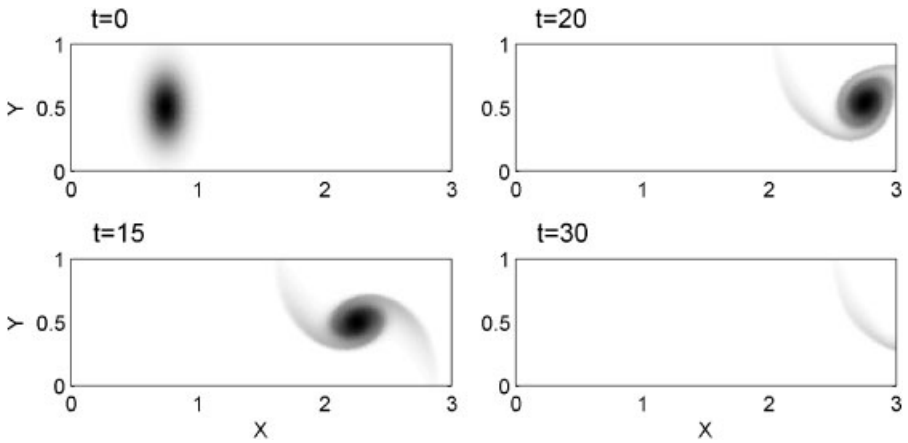

Figure 8. Vortex patch at various moments of time t for $Q_1 = 0.1$.

4.1. Washing out of the vortex patch from the channel

Consider first $Q_1 = 0.1$ which corresponds to the upper end of the range of the inlet velocities considered here. The results of the calculations of the evolution of a vortex patch are shown in Figure 8. One can see that the vortex patch is quickly carried away from the channel. The time interval for which all initial fluid particles are washed out of the channel is $30.9 \approx L/v^w$. This means that the presence of an initial vortex patch practically does not affect the length of this time interval. As a result, for large times we obtain the asymptotically stable steady flow (11) without stagnation zones, and this is in agreement with the known theoretical results [9]. At the same time, this result gives us an additional confirmation of the validity of the numerical method employed. For the time interval during which the vortex patch remains in the channel, the form of the patch does not have enough time to change considerably. Within this time interval there are only small smooth variations in the maximum velocity in the channel with a small rise in the maximum velocity when the vortex patch approaches the outlet (see Figure 6,(b)). The trajectory of the particle that carries the maximum vorticity (see Figure 7) is almost parallel to the x-axis at the initial stage of the evolution and moves towards the upper wall of the channel only when the particle is sufficiently close to the outlet.

4.2. Slowing down of the washing out of the vortex patch

If the inlet velocity is reduced, the presence of an initial vortex patch starts to affect the time of the total washing out (the length of the time interval for which all initial fluid particles are washed out of the channel). The dynamics of the vortex patch for $Q_1 = 0.035$ is shown in Figure 9. In this case the time of the total washing out is 96.8. Thus, the presence of an initial vortex patch leads to an increase in the total washing out time by 13% (relative to the total washing out time of infinitesimal perturbations by the steady flow (11), which is equal to $L/v^w = L/Q_1$).

The dynamics of the vortex patch at the initial stages of the evolution is similar in all cases considered here (see Figures 8, 9, 11), but can be quite different near the outlet of the channel. The difference in behaviour at the initial stages is determined by the parameter Q_1: the smaller it is (i.e. the smaller the inlet velocity is), the more significant the subsequent changes in the vortex

Copyright © 2008 John Wiley & Sons, Ltd.

DOI: 10.1002/fld

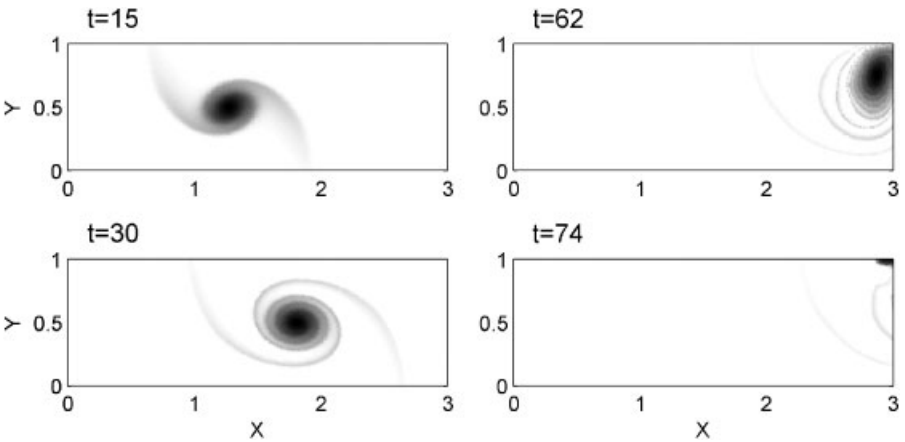

Figure 9. Vortex patch at various moments of time t for $Q_1 = 0.035$.

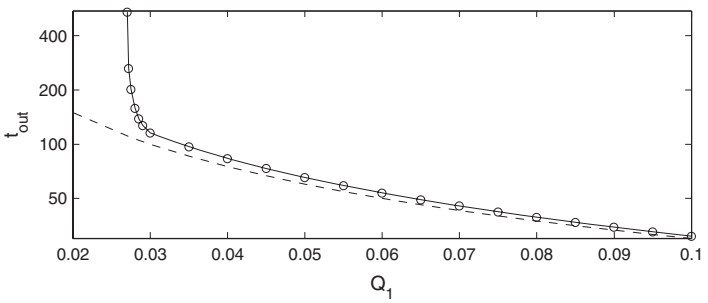

Figure 10. The washing out time of vortex patch versus Q_1. The total washing out time of infinitesimal perturbations by the steady flow (11) is shown by dashed curve. For $Q_1 = 0.1$, $t_{\text{out}} = 30.9 \approx L/v^w$.

patch form are. It can be clearly demonstrated by comparing the fields of vorticity for the same moments of time t and for different values of parameter Q_1, e.g. for $Q_1 = 0.1, 0.035$ at $t = 15$ (Figures 8, 9) or for $Q_1 = 0.035, 0.02$ at $t = 30$ (Figures 9, 11).

When the vortex patch approaches the outlet (for $Q_1 = 0.04, 0.03$), it moves towards the upper wall of the channel. This is clearly demonstrated by the trajectories of the centre of the vortex patch shown in Figure 7. Note that the vortex patch moves close to the upper right corner of the D and remains there for some time, and this increases the total washing out time (see Figure 9). Figure 6(b) shows that when the vortex patch approaches the outlet, there is a local (in time) peak in the maximum velocity. Nevertheless, in both cases considered in this subsection, the final result of the flow evolution is the steady regime with no stagnation zones (11).

The fact that when Q_1 decreases the total washing out time increases is clearly seen in Figure 10, which shows the total washing out time t_{out} versus Q_1. The total washing out time of (infinitely) small initial perturbations by the steady flow (11), which is equal to L/Q_1, is also shown in Figure 10 (dashed curve). Evidently, the curve $t_{\text{out}}(Q_1)$ approaches a vertical asymptote at $Q_1 \approx 0.0269$. This indicates that the behaviour of the vortex patch for $Q_1 < 0.0269$ is qualitatively different from its behaviour for $Q_1 > 0.0269$.

Copyright © 2008 John Wiley & Sons, Ltd.

DOI: 10.1002/fld

4.3. Formation of a flow with stagnation zones

The situation changes completely for $Q_1 < 0.0269$. Here, we will describe in detail the case $Q_1 = 0.02$ (see Figure 11). First, the vortex patch moves to the right and comes close to the outlet at $t \approx 115$. Then the larger, most intense part of the vortex moves up towards the upper wall and then starts moving back (to the left), whereas some parts of the vortex are washed out of the channel. After that, the value of the integral of the vorticity over the flow domain I_ω remains practically unchanged (see. Figure 6(a)).

When the vortex patch reaches the left side of the rectangle (the inlet) (at $t \approx 280$) it starts to move to the right again. Then, the same motion is repeated each time the spatial amplitude of this motion decreases (see Figure 11 $t = 115, 515, 2000, 5000$). All stages of the evolution of the vortex patch are shown in Figure 11. As a result of a long-time numerical simulation, we approach

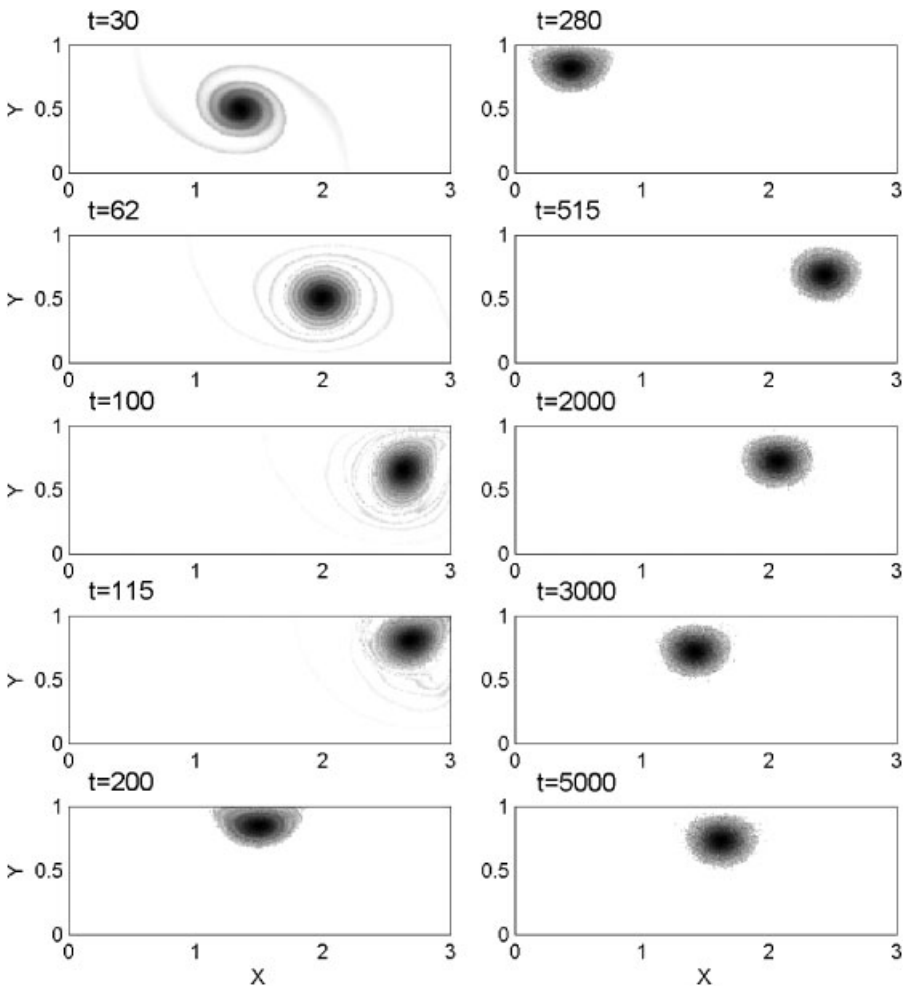

Figure 11. Vortex patch at various moment of time t for $Q_1 = 0.02$.

Copyright © 2008 John Wiley & Sons, Ltd.

DOI: 10.1002/fld

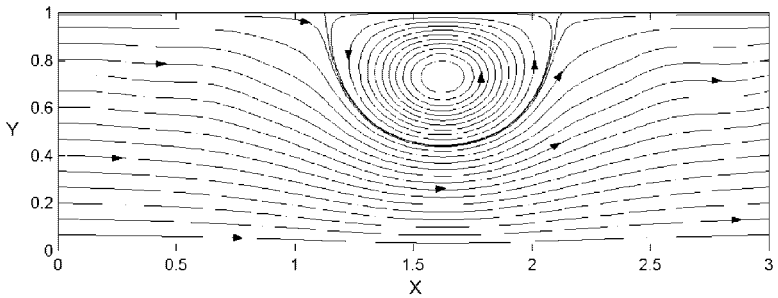

Figure 12. Streamlines of the steady regime.

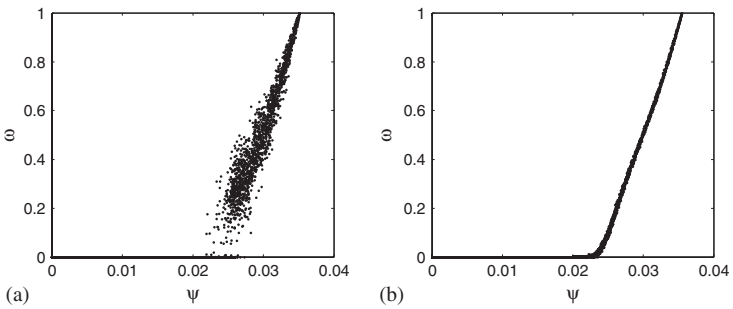

Figure 13. Vorticity versus stream function: (a) steady regime appearing as a final state of unsteady evolution of the initial vortex patch and (b) a numerical steady solution of the Euler equations that is close to the regime (a).

a regime that is close to a steady one. Thus, we observe the relaxation to a steady regime, i.e. the behaviour which is usually associated with dissipative systems. This is clearly illustrated by the corresponding trajectory of the centre of the vortex patch in Figure 7.

The regime that appears as a result of a long-time unsteady evolution of the initial vortex patch is shown in Figure 11 for $t=5000$, the corresponding streamlines are shown in Figure 12. It is known that in a steady flow of an inviscid incompressible fluid, vorticity ω and stream function ψ are functionally dependent. For the flow presented in Figure 11 for $t=5000$, the vorticity versus the stream function is shown in Figure 13(a). One can see that the relationship between the vorticity and the stream function is close to functional, although there are perturbations in the part of the graph that corresponds to the boundary of the vortex patch. This is a consequence of the numerical errors accumulated in the course of a long-time computation, which is required to obtain the steady regime. To find a steady solution of the Euler equations, which is close to the above steady regime, we employ the averaging and filtration procedure described in Section 2. As a result, we obtain a steady flow with the streamlines, which is almost the same as those shown in Figure 12 and with the functional relationship between ω and ψ shown in Figure 13(b). This steady regime is very likely to be stable, as during a long-time numerical calculation of the unsteady problem with the initial conditions corresponding to this regime the flow remains practically unchanged (in the interval $t\in[0,1000]$, the errors in all controlled quantities do not exceed 0.01%).

Copyright © 2008 John Wiley & Sons, Ltd.

DOI: 10.1002/fld

Thus, for small inlet velocity v^w we observe the formation of a steady regime with a stagnation zone.

Similar behaviour of the vortex patch takes place for all Q_1 from the interval $0<Q_1<0.0269$. The only difference between these similar regimes is the time of relaxation of the initial vorticity distribution to the steady regime. This time grows when Q_1 decreases. In the absence of flow through the domain, i.e. for $Q_1=0$, there is no dissipation and there is no relaxation to a steady regime. In this case, non-decaying motions of the vortex patch occur, as can be seen in Figure 7, and these motions are accompanied by changes in the shape of the (originally) elliptic vortex, which are similar to the changes of the vortex patch shape shown in Figure 4.

5. CONCLUSION

We have proposed a numerical scheme for the numerical simulations of two-dimensional unsteady inviscid incompressible flows through a rectangular domain in the case when the normal component of velocity is given both at the inlet and the outlet and the vorticity is specified at the inlet. The proposed numerical scheme has been tested on a number of examples. These and some other calculations are in good agreement with known theoretical results: the washing out of small perturbations for finite time, the persistence of unsteady motions in the case of no flow through the domain, and the conservation of the integral of the vorticity over the flow domain in all steady regimes. In addition, the results presented in the paper do not change qualitatively if we use a refined approximation (higher number of particle, more cells, etc.).

The proposed numerical scheme has been employed to analyze the dynamics of the washing out of an initial vortex patch in a channel of finite length. The simplest situation has been considered: the constant velocity at the inlet and the outlet and zero vorticity at the inlet. We have investigated the dependence of the dynamics of the initial vortex patch on the velocity at the inlet. It turned out that if the inlet velocity is high enough, the vortex patch is completely washed out of the flow domain in finite time, after which we observe asymptotically stable plane parallel flow. This is in complete agreement with theoretical results [9]. When the inlet velocity decreases, the time interval within which the vortex patch remains in the channel increases, and there is a critical value of the inlet velocity below, which a part of the vortex patch remains in the channel forever. It has been shown by solving the unsteady problem numerically for a long-time interval that as $t\to\infty$ the flow approaches to a regime, which is close to a steady vorticity distribution. To obtain a steady flow, we applied the procedure of spatial averaging and filtration (described in Section 2) to the vorticity distribution obtained by a long-time computation of the unsteady problem. As a result, we were able to compute the vorticity distribution that corresponds to a steady flow with stagnation zones.

Thus, we have shown that in the problem considered there are non-trivial steady flows with stagnation (recirculation) zones, which appear to be asymptotically stable (which, in turn, is possible due to dissipation). Such regimes can be realized in channels of finite length when the inlet velocity is small and the intensity of the initial vortex is sufficiently large. This represents the main result of the present study.

Similar studies have been carried out for other profiles of the velocity at the inlet and outlet, which correspond to the classical Couette and Pouiselle flows. These studies have produced similar results and are not presented here. In all cases, for a sufficiently small inlet velocity, the evolution of an initial vortex patch results in appearance of a steady flow with stagnation zones.

Copyright © 2008 John Wiley & Sons, Ltd.

DOI: 10.1002/fld

ACKNOWLEDGEMENTS

Some calculations presented in this paper used the computer facilities of the HIVE laboratory (Hull Immersive Visualization Environment) University of Hull (U.K.). This work was done in the framework of European research group 'Regular and chaotic hydrodynamics'. It was also supported by EPSRC Research Grant GR/S96616/02 and by CRDF grant RUM1-2842-RO-06.

REFERENCES

1. Kochin NE. On the existence theorem in hydrodynamics. *Prikladnaya Mathematica i Mekhanika* 1956; **20**(2): 153–172. (Translated in Journal of Applied Mathematics and Mechaniks ISSN 0021-8928.)
2. Yudovich VI. A two-dimensional non-stationary problem on the flow of an ideal incompressible fluid through a given region. *Matematicheskii Sbornik* (*N.S.*) (Russian) 1964; **64**(106):562–588.
3. Kazhikhov AV. Note on the formulation of the problem of flow through a bounded region using equations of perfect fluid. *Journal of Applied Mathematics and Mechanics* 1980; **44**(5):672–674.
4. Alekseev GV. Vanishing viscosity in two-dimensional stationary problems of the hydrodynamics of an incompressible fluid. *Dinamika Splošn. Sredy Vyp.* (Russian) 1972; **10**:5–25, 246.
5. Elcrat A, Fornberg B, Horn M, Miller K. Some steady vortex flows past a circular cylinder. *Journal of Fluid Mechanics* 2000; **409**:13–27.
6. Elcrat AR, Miller KG. Free surface waves in equilibrium with a vortex. *European Journal of Mechanics-B/Fluids* 2006; **25**(2):255–266.
7. Saffman PG. *Vortex Dynamics*. Cambridge Monographs on Mechanics and Applied Mathematics. Cambridge University Press: Cambridge, 1992.
8. Lee TS, Liao W, Low HT. Numerical simulation of turbulent flow through series stenoses. *International Journal for Numerical Methods in Fluids* 2003; **42**(7):717–740.
9. Morgulis A, Yudovich V. Arnold's method for asymptotic stability of steady inviscid incompressible flow through a fixed domain with permeable boundary. *Chaos* 2002; **12**(2):356–371.
10. Moshkin NP, Mounnamprang P. Numerical simulation of vortical ideal fluid flow through curved channel. *International Journal for Numerical Methods in Fluids* 2003; **41**(11):1173–1189.
11. Cottet G-H, Koumoutsakos PD. *Vortex Methods*: *Theory and Practice*. Cambridge University Press: Cambridge, 1999.
12. Ould-Salihi ML, Cottet G-H, El Hamraoui M. Blending finite difference and vortex methods for incompressible flow computations. *SIAM Journal on Scientific Computing* 2000; **22**(5):1655–1674.
13. Hald O. Convergence of vortex methods, II. *SIAM Journal on Numerical Analysis* 1979; **16**:726–755.
14. Beale JT, Majda A. Vortex methods II: higher order accuracy in two and three dimensions. *Mathematics of Computation* 1982; **39**:29–52.
15. Anderson C, Greengard C. On vortex methods. *SIAM Journal on Numerical Analysis* 1985; **22**(3):413–440.
16. Koumoutsakos P. Inviscid axisymmetrization of an elliptical vortex. *Journal of Computational Physics* 1997; **138**(2):821–857.
17. Strain J. 2D vortex methods and singular quadrature rules. *Journal of Computational Physics* 1996; **124**(1):131–145.
18. Antontsev SN, Kazhikhov AV, Monakhov VN. *Boundary Value Problems in Mechanics of Nonhomogeneous Fluids* [translated from the Russian]. Studies in Mathematics and its Applications, vol. 22. North-Holland: Amsterdam, 1990.
19. Xu C, Maday Y. A spectral element method for the time-dependent two-dimensional Euler equations: applications to flow simulations. *Journal of Computational and Applied Mathematics* 1998; **91**:63–85.
20. Chacon Vera E, Chacon Rebollo T. On cubic spline approximations for the vortex patch problem. *Applied Numerical Mathematics* 2001; **36**:359–387.
21. McLachlan R. Area preservation in computational fluid dynamics. *Physics Letters A* 1999; **264**:36–44.
22. Sanz-Serna JM, Calvo MP. *Numerical Hamiltonian Problems*. Chapman & Hall: London, 1994.
23. Aubry A, Chartier P. Pseudo-symplectic Runge–Kutta methods. *BIT* 1998; **38**(3):439–461.
24. Aubry A, Chartier P. A note on pseudo-symplectic Runge–Kutta methods. *BIT* 1998; **38**(4):802–806.
25. Schecter DA, Dubin DHE, Cass AC, Driscoll CF, Lansky IM, O'Neil TM. Inviscid damping of asymmetries on a two-dimensional vortex. *Physics of Fluids* 2000; **12**(10):2397–2412.

Copyright © 2008 John Wiley & Sons, Ltd.

DOI: 10.1002/fld